THE BRIGHT OPTICAL COMPANION TO THE ECLIPSING MILLISECOND PULSAR IN NGC 6397

Francesco R. Ferraro, Andrea Possenti, Nichi D'Amico, and Elena Sabbi

Osservatorio Astronomico di Bologna, via Ranzani 1, I-40127 Bologna, Italy

ABSTRACT

We report the optical identification of the companion to the eclipsing millisecond pulsar PSR J1740−5340 in the globular cluster NGC 6397. A bright variable star with an anomalous red color and optical variability (∼0.2 mag) that nicely correlates to the orbital period of the pulsar (∼1.35 days) has been found close to the pulsar position. The peculiar shape of the optical light curves is unprecedented for a millisecond pulsar companion and is a clear signature of tidal distortions.

Subject headings: binaries: close — globular clusters: individual (NGC 6397) — pulsars: individual (PSR J1740−5340) — stars: evolution — stars: mass loss — stars: neutron

1. INTRODUCTION

The millisecond pulsar (MSP) PSR J1740−5340 was discovered during a systematic search of the Galactic globular cluster (GC) system for millisecond pulsars, carried out with the Parkes radio telescope (D'Amico et al. 2001a, 2001b). The pulsar, associated with the GC NGC 6397, is member of a binary system with a relatively wide orbit of period ≃1.35 days, and it is eclipsed for about 40% of the orbit at 1.4 GHz. In a companion Letter, D'Amico et al. (2001c) provide strong evidence that the companion star could be an unusual object and give a precise position for the pulsar. We here present the results of a search of the optical companion to PSR J1740−5340 in the *Hubble Space Telescope* (*HST*) archive.

2. OBSERVATIONS AND DATA ANALYSIS

The photometric data consist of a series of public *HST* exposures taken in 1996 March and 1999 April, retrieved from the ESO/ST-ECF Science Archive. The 1999 observations consist of 116 Wide Field Planetary Camera 2 (WFPC2) exposures with filters F555W, F675W, F814W, and F656N (referred to here as V_{555}, R_{675}, I_{814}, and Hα), spanning about 1.8 days. The 1996 observations consist of 55 exposures with filters F336W and F439W (referred to here as U_{336} and B_{439}), spanning 0.4 and 0.2 days, respectively. The position derived from pulse timing (R.A. = $17^h40^m44{\overset{s}{.}}589$, decl. = $-53°40'40{\overset{''}{.}}9$) is 29″ east and 16″ south of the cluster center (Djorgovski & Meylan 1993). We used the STSDAS program METRIC to roughly locate the MSP in the retrieved WFPC2 images, and it is on the WF4 chip in both data sets.

The exact location of the MSP in the *HST* images was obtained by searching an astrometric solution for a wide-field CCD image of a region around NGC 6397. We retrieved from the ESO Science Archive an image obtained in 1999 May with the Wide-Field Imager (WFI) at the ESO 2.2 m telescope (at the European Southern Observatory, La Silla, Chile). The entire image consists of a mosaic of eight chips (each with a field of view of 8′ × 16′) giving a global field of view of 33′ × 34′. Only the chip containing the cluster center was used. The new astrometric Guide Star Catalog (GSCII) was used to search for astrometric standard lying in the WFI image field of view: several hundred astrometric GSCII reference stars have been found, allowing an accurate absolute positioning of the image.

In order to derive an astrometric solution for the WFI image, we used a procedure developed at the Bologna Observatory.

The resulting rms residuals were on the order of ∼0″.3 in both right ascension and declination. By using this astrometry, we were able to accurately locate the nominal position of the MSP in the WFI image and in the *HST* WFPC2 images.

The bottom right panel in Figure 1 shows an enlargement of a 7″ × 7″ region of the WF4 chip, centered on the MSP position. The 3 σ error circle, which takes into account the global error in the absolute positioning of the MSP, is shown. The global error is fully dominated by the uncertainty due to the astrometric procedure. One relatively bright star (A) is within the error box of the MSP. Two additional objects (B and C) are just outside the error circle. In order to investigate the nature of these objects, we performed photometric analysis of the entire *HST* WFPC2 data set retrieved from the archive.

The photometric reductions have been carried out using ROMAFOT (Buonanno et al. 1983), a package developed to perform accurate photometry in crowded fields and specifically optimized to handle undersampled point-spread function (PSF), as in the case of the *HST* WF chips (Buonanno & Iannicola 1989). The standard procedure described in Ferraro et al. (1997) was adopted in order to derive PSF-fitting instrumental magnitudes, which were finally calibrated using zero points listed by Holtzman et al. (1995). In particular, we used a sample of median-combined images to construct reference color-magnitude diagrams (CMDs). The three remaining panels in Figure 1 show multiband CMDs for stars detected in a region of 400 × 400 pixels (corresponding to 40″ × 40″): the locations of the three objects are indicated.

The results of the PSF fitting procedure for these stars have been carefully examined by visual inspection. From this accurate photometric analysis, we found that the bright object A lying within the error box of the MSP has an anomalous position in the CMD since it is located at the luminosity of the main-sequence (MS) turnoff region but it has an anomalous red color; the other two objects (B and C) are normal MS stars. Individual images were instead used to check the variability of the objects. Objects B and C show no significant time variability compared to the measurement uncertainties. On the other hand, object A shows a remarkable time modulation (∼0.2–0.3 mag) on a scale of several hours. This object is the variable star WF 4-1 discovered by Taylor et al. (2001), who noted its optical variation and measured a modulation period. On the basis of the unusual colors and time variability, Taylor et al. (2001) have classified this object as a BY Draconis star.

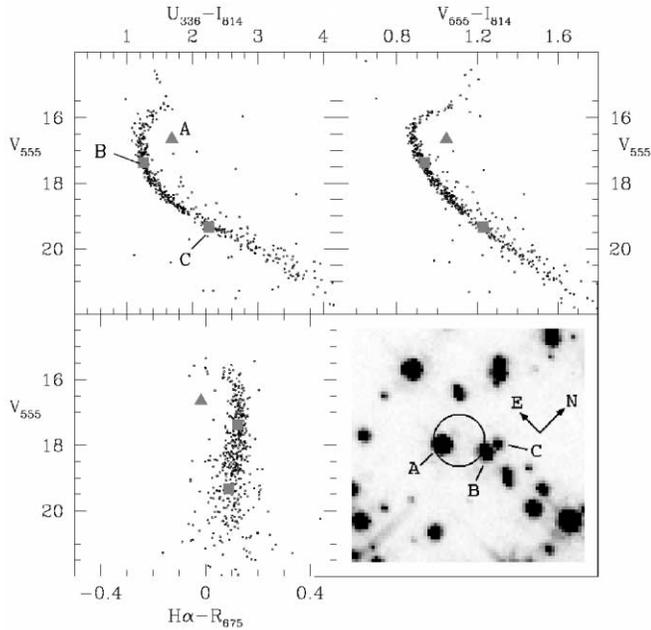In order to check the association of the time variability of

FIG. 1.—*Bottom right panel*: Portion of a median-combined F675W *HST* WFPC2 image (chip WF4) of NGC 6397, centered near the MSP position. The region covers about $7'' \times 7''$. Star A is the proposed companion to the MSP PSR J1740−5340. *Remaining panels*: Multiband CMDs for stars detected in a region of the WF4 chip ($40'' \times 40''$) containing the MSP position. The three stars found in the vicinity of the MSP error box are marked with different symbols (a triangle for star A and squares for stars B and C) and labeled with their names in the first panel.

star A to the pulsar binary motion, we have carried out a detailed time analysis. The data available consist of four time series in the $H\alpha$, R_{675}, I_{814}, and V_{555} bands taken in 1999, spanning ~1.8 days, and two time series in the B_{439} and U_{336} bands taken in 1996, spanning 0.2 and 0.4 days, respectively. The $H\alpha$-band time series were processed using GRATIS (GRAphycal Analyzer of TIme Series), a software package developed at the Bologna Astronomical Observatory (see, for instance, Clementini et al. 2000). In the GRATIS χ^2 FITTING routine, the amplitude and phase of up to n_h harmonics of a truncated Fourier series are fitted to the data, and the resulting χ^2 is plotted as a function of the modulation period of each template. Being based on a fitting procedure, this method is different from the popular Lomb-Scargle periodogram (Scargle 1982). As pointed out by Faulkner (1977), the fitting method is more reliable for short data spans (comparable to the data span length), and use of multiple harmonics allows increased sensitivity to signals that are not strictly sinusoidal. When several cycles of a given periodicity are available, the two methods are almost equivalent. As already mentioned, the data span of the $H\alpha$-band time series is ~1.8 days, and the searched periodicity is 1.35 days, so the χ^2 fitting method is largely preferable.

Figure 2 shows the reduced χ^2 resulting from the fitting of the $H\alpha$ data as a function of the modulation period for $n_h =$ 2. The most significant feature is indeed a periodicity around the radio period of 1.35 days, with substantial power also near the second harmonic. The confidence level peak (99.6%) corresponds to a period $P = 1.37 \pm 0.05$ days (consistent, within the uncertainties, with the period quoted by Taylor et al. 2001 for the WF 4-1 variable). The quoted uncertainty corresponds to the period range for which the confidence level is larger than 99%, and it is dominated by the relatively short (~1.8 days) data span available. Although the statistical significance of the fit is
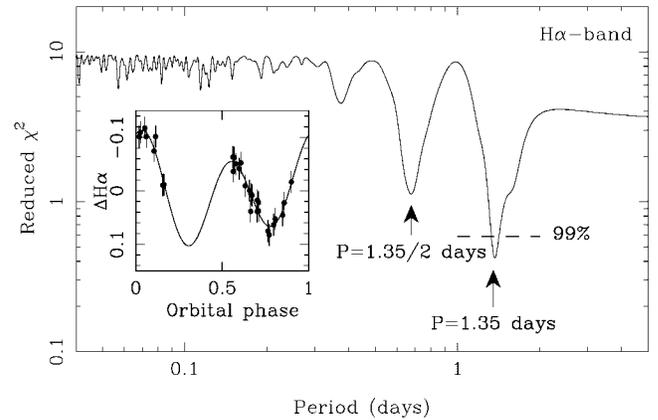
not very high (~99%), it strongly suggests that the variability of star A is associated to the pulsar binary motion.

Prompted by this evidence, we have then phased the same $H\alpha$ data using the period P and the reference epoch T_0 of the radio ephemeris and have fitted the spectral amplitudes of the first and second harmonics to the resulting light curve. The best fit, shown in the inset in Figure 2 as a solid line, is not what we would expect on the basis of a simple pulsar irradiation model, as we will discuss in § 3. The time variability observed in the R, I, and V bands at the same epochs follows a similar pattern to that observed in the $H\alpha$ band. Figure 3 shows the same $H\alpha$-band data and U_{336}-band data taken in 1996, phased using the accurate radio ephemeris. Remarkably, the two data sets show the minimum at the same orbital phase, giving further evidence that the optical modulation is indeed associated to the pulsar binary motion.
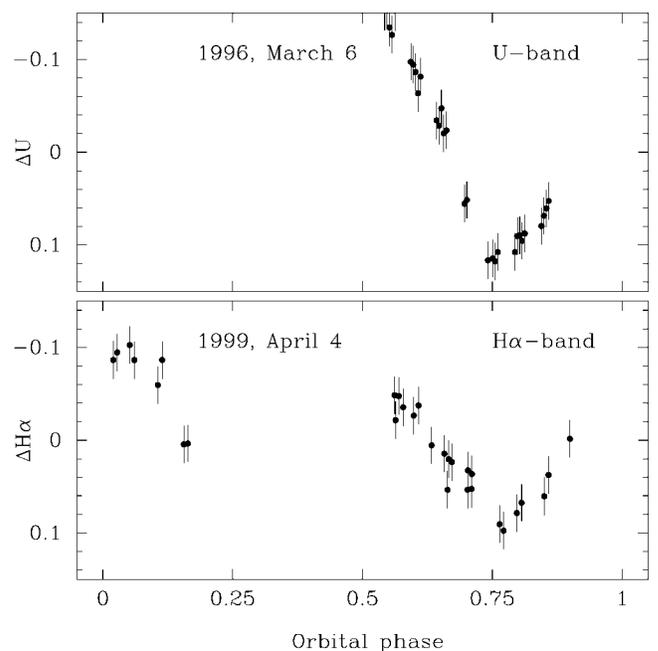

FIG. 2.—Reduced χ^2 resulting from the fit of two Fourier harmonics to the $H\alpha$ data as a function of the modulation period. *Inset*: Same $H\alpha$ data folded using the period and the reference epoch of the radio ephemeris, and best fit (*solid line*) of the spectral amplitudes of the first and second harmonics to the data.

FIG. 3.—$H\alpha$ data and U_{336} data taken 3 yr apart, phased using the radio ephemeris.

Further support to the proposed association derives from the detection of X-ray emission from the MSP in a *Chandra* pointing of NGC 6397 (Grindlay et al. 2001). Using the very likely identifications of cataclysmic variables, the *Chandra* and *HST* frames have been tied to ~0″.1, which in turn ties the X-ray, optical, and radio positions to the same precision.

3. OBSERVED PROPERTIES OF THE COMPANION STAR

In the radio timing paper, D'Amico et al. (2001c) demonstrate that the companion star cannot be the typical white dwarf (WD) found in most binary MSPs. They propose that the companion may be an MS star acquired by exchange interaction in the cluster core or, alternatively, it may be the same star that spun up the MSP, in which case it may still be overflowing its Roche lobe. Assuming that star A is the pulsar companion, we here discuss these two hypotheses, comparing them with observed optical properties of star A.

In order to get some quantitative hints on the effective temperature T_{eff} and the radius R_c of star A, we used the recent set of isochrones by Silvestri et al. (1998) and by VandenBerg (2000). By comparing the CMDs in Figure 1 with those isochrones, for metallicity [Fe/H] = −2.00 and ages of t = 12–14 Gyr (compatible with the values measured for NGC 6397), we derive $R_c \sim$ 1.3–1.8 $R_\odot$ and $T_{eff} \sim$ 5500–5800 K for star A. The given intervals in R_c and T_{eff} account for both the flux and color variations of star A and the uncertainties in matching our CMDs with the isochrones.

The peculiar nature of star A can be unveiled by inspecting the amplitude and the shape of its light curves (Fig. 2). Two other eclipsing MSPs, both in the Galactic field, have measured light curves: PSR B1957+20 (Callanan, van Paradijs, & Rengelink 1995) and PSR J2051−0827 (Stappers et al. 2001). In both cases, the optical companions show strong modulations, which are readily explained by the heating of one side of the companion by radiation from the pulsar. The optical maximum is at orbital phase 0.75, where the heated side of the companion faces the Earth. A similar trend, although with a much smaller degree of modulation, is seen in 47 Tuc U_{opt}, the first identified MSP companion in a GC (Edmonds et al. 2001).

The light curves of star A are completely different. We locate the phase 0.0 at the ascending node of the MSP orbit; thus, at the phase 0.75 we see the side of the companion facing the pulsar. In contrast to the other known variable MSP companions, the light curves of star A display there a minimum instead of a maximum (see Fig. 2). Within the limits in the orbital period coverage of our photometry, the best-fit light curve of Figure 2 shows two maxima and two minima during each binary orbit: thus, tidal distortions appear more responsible for this pattern. Such deformations of the stellar shape have been invoked to explain the light curves of the optical companions to black hole candidates (van der Klis et al. 1985) and neutron stars (NSs; Zurita et al. 2000). In this scenario, the maxima correspond to quadratures (phases 0.0 and 0.50) when the distorted star presents the longest axis of its ellipsoid to the observer, the minima to the conjunctions. It is easy to recognize this trend in the inset of Figure 2.

If this is the correct interpretation, it results in severe constraints on the mass and the nature of star A. The degree of ellipsoidal variations depends roughly on (Russell 1945) $\Delta m = k_\lambda (M_{MSP}/M_c)(R_L/a)^3 F^3 \sin^2 i$, where M_{MSP} and M_c are the masses of the MSP and its companion, R_L is the Roche lobe radius of the companion, a is the orbital separation, F is the ratio between the average radius of the star and the Roche lobe

radius, and i is the inclination of the orbit. The term $k_\lambda = 2.6$ accounts for limb and gravity darkening for Hα radiation from our source (Lucy 1966). Given the orbital parameters of PSR J1740−5340 (D'Amico et al. 2001c), it follows that $(M_{MSP}/M_c)(R_L/a)^3 \sim 0.07$ for all the possible companions, and thus $\Delta m_{H\alpha} \lesssim 0.2 F^3 \sin^2 i$. The observed modulation (Fig. 2, *inset*) is just ~0.2 mag; that can be reproduced only if the companion has almost filled up its Roche lobe ($F \sim 1$) and the orbital plane is nearly edge-on ($i \sim 90°$). Remarkably, these two requirements are contemporarily accomplished by a companion of mass in the range 0.19–0.22 $M_\odot$, whose Roche lobe radius (1.32–1.42 $R_\odot$) just matches the lower limit inferred for the observed radius R_c of star A .

The light curve of a star affected only by tidal distortion would have the minimum at phase 0.25 less deep than that at phase 0.75. The reversal of this rule in the case of star A can result from the overheating of the side facing the pulsar. In contrast to 47 Tuc U_{opt} and to the companions to PSR J2051−0827 and to PSR B1957+20, the larger orbital separation and/or the greater value of F for star A allow ellipsoidal variations to dominate over the thermal modulation.

4. DISCUSSION

In summary, this system is the first example of a binary MSP in which the optical light curve of the companion shows tidal distortions, providing strong evidence that the MSP is orbiting a companion whose Roche lobe is completely filled. The optical brightness of such a companion would allow unprecedented detailed investigations, for example, about the origin of this system.

A first hypothesis is that star A is an MS star perturbed by the energetic flux emitted from the MSP. The so-called *illumination* mechanism (D'Antona 1995) predicts that if the heating luminosity $L_h \lesssim \frac{1}{4}(R_*/a)^2 L_{irr}$ (where R_* is the star radius and L_{irr} the MSP luminosity) is large enough, the star inflates and increases the effective temperature, thus modifying its photometric characteristics (Podsiadlowski 1991). The rotational energy loss from the MSP is $L_{irr} \sim 1.4 \times 10^{35}$ ergs s^{-1} (D'Amico et al. 2001c). At the distance $a \sim 6.5$ $R_\odot$, this corresponds to a characteristic temperature for the heating bath in which the star is immersed of $T_h = [1/(16\sigma\pi)L_{irr}/a^2]^{1/4} \lesssim 4000$ K, where σ is the constant of Stefan-Boltzmann. We expect that the MSP flux significantly affects the companion only if $T_h \gtrsim T_*$ (where T_* is the effective temperature of an unperturbed MS star), and $T_* \lesssim 4000$ K implies $\lesssim 0.4$ $M_\odot$. As T_h does not depend on R_*, it seems energetically difficult to explain an increasing of ~40% of the effective temperature; however, only detailed simulations of the system will allow us to assess if such a low-mass MS star of radius ~0.2–0.4 $R_\odot$ can indeed be bloated up to $\lesssim 1.3$ $R_\odot$ and heated from ~4000 to ~5500 K by the energetic flux of the MSP.

Another fascinating possibility is that PSR J1740−5340 is a newborn MSP, the first one observed just after the end of the process of recycling. In this case (L. Burderi, F. D'Antona, & M. Burgay 2001, in preparation), star A could have been originally an MS star of ~1 $M_\odot$ whose evolution triggered mass transfer toward the compact companion, spinning it up to millisecond periods (Alpar et al. 1982). Irregularities in the mass transfer rate from the companion, $\dot{M}_c$, are common in the evolution of these systems (e.g., Tauris & Savonije 1999): even a short decreasing of $\dot{M}_c$ can have easily allowed PSR J1740−5340 (having a magnetic field ~8 × 10^8 G and a rotational period $\lesssim 3.65$ ms) to become source of relativistic par-

ticles and magnetodipole emission, whose pressure (1) first swept the environment of the NSs, allowing coherent radio emission to be switched on (Shvartsman 1970), and (2) then kept on expelling the matter overflowing from the Roche lobe of star A (Ruderman, Shaham, & Tavani 1989). For a wide enough binary system (as is the case of PSR J1740−5340), once the radio pulsar has been switched on, any subsequent restoration of the original $\dot{M}_c$ cannot quench the radio emission (Burderi et al. 2001). In this case, we have now a donor star still losing matter from its Roche lobe at $\dot{M}_c \gtrsim 5 \times 10^{-11}\ M_\odot\ \mathrm{yr}^{-1}$ (D'Amico et al. 2001c; a high mass-loss rate, difficult to explain in the model of a bloated star). At the same time, accretion on the NS is inhibited because of the pressure exerted by the pulsar on the infalling matter. This strong interaction between the MSP flux and the plasma wind would explain also the irregularities seen in the radio signals from PSR J1740−5340, sometimes showing the presence of ionized matter along the line of sight even when the pulsar is between star A and the observer. The characteristic age of PSR J1740−5340 (~3.5 × 10^8 yr) would indicate that it is a young MSP, further supporting this scenario.

If star A will continue releasing matter at the present rate, $\dot{M}_c$, PSR J1740−5340 is not a candidate for becoming an isolated pulsar. When star A will have shrunk well inside its Roche lobe, the system will probably end up as MSP + WD (or a light nondegenerate companion). If star A will undergo a significant increasing of $\dot{M}_c$, the condition for the accretion could be reestablished and PSR J1740−5340 would probably appear again as a low-mass X-ray binary or as a soft X-ray transient (Campana et al. 1998).

REFERENCES

Alpar, M. A., Cheng, A. F., Ruderman, M. A., & Shaham, J. 1982, Nature, 300, 728

Buonanno, R., Buscema, G., Corsi, C. E., Ferraro, I., & Iannicola, G. 1983, A&A, 126, 278

Buonanno, R., & Iannicola, G. 1989, PASP, 101, 294

Burderi, L., et al. 2001, ApJ, 560, L71

Callanan, P. J., van Paradijs, J., & Rengelink, R. 1995, ApJ, 439, 928

Campana, S., Colpi, M., Mereghetti, S., Stella, L., & Tavani, M. 1998, A&A Rev., 8, 279

Clementini, G., et al. 2000, AJ, 120, 2054

D'Amico, N., Lyne, A. G., Manchester, R. N., Possenti, A., & Camilo, F. 2001a, ApJ, 548, L171

D'Amico, N., Possenti, A., Manchester, R. N., Sarkissian, J., Lyne, A. G., & Camilo, F. 2001b, in Proc. 20th Texas Symp. on Relativistic Astrophysics (New York: AIP), in press (astro-ph/0105122)

———. 2001c, ApJ, 561, L89

D'Antona, F. 1995, in Evolutionary Processes in Binary Stars, ed. R. A. M. Wijers, M. B. Davies, & C. A. Tout (NATO ASI Ser. C, 477; Dordrecht: Kluwer), 287

Djorgovski, S., & Meylan, G. 1993, in ASP Conf. Ser. 50, Structure and Dynamics of Globular Clusters, ed. S. G. Djorgovski & G. Meylan (San Francisco: ASP), 325

Edmonds, P. D., Gilliland, R. L., Heinke, C. O., Grindlay, J. E., & Camilo, F. 2001, ApJ, 557, L57

Faulkner, D. J. 1977, ApJ, 216, 49

Ferraro, F. R., et al. 1997, A&A, 324, 915

Grindlay, J. E., Heinke, C. O., Edmonds, P. D., Murray, S. S., & Cool, A. M. 2001, ApJL, submitted (astro-ph/0108265)

Holtzman, J. A., Burrows, C. J., Casertano, S., Hester, J. J., Trauger, J. T., Watson, A. M., & Worthey, G. 1995, PASP, 107, 1065

Lucy, L. B. 1966, Z. Astrophys., 65, 89

Podsiadlowski, P. 1991, Nature, 350, 136

Ruderman, M., Shaham, J., & Tavani, M. 1989, ApJ, 336, 507

Russell, H. R. 1945, ApJ, 102, 1

Scargle, J. D. 1982, ApJ, 263, 835

Shvartsman, V. F. 1970, Radiofizika, 13, 1852

Silvestri, F., Ventura, P., D'Antona, F., & Mazzitelli, I. 1998, ApJ, 509, 192

Stappers, B. W., van Kerkwijk, M. H., Bell, J. F., & Kulkarni, S. R. 2001, ApJ, 548, L183

Tauris, T. M., & Savonije, G. J. 1999, A&A, 350, 928

Taylor, J. M., Grindlay, J. E., Edmonds, P. D., & Coll, A. M. 2001, ApJ, 553, L169

VandenBerg, D. A. 2000, ApJS, 129, 315

van der Klis, M., Clausen, J. V., Jensen, K., Tjemkes, S., & van Paradijs, J. 1985, A&A, 151, 322

Zurita, C., et al. 2000, MNRAS, 316, 137